

Onset of colored-noise-induced synchronization in chaotic systems

Yan Wang,^{1,2} Ying-Cheng Lai,^{1,3} and Zhigang Zheng²

¹*Department of Electrical Engineering, Arizona State University, Tempe, Arizona 85287, USA*

²*Department of Physics, Beijing Normal University, Beijing 100875, China*

³*Department of Physics, Arizona State University, Tempe, Arizona 85287, USA*

(Received 11 December 2008; published 12 May 2009)

We develop and validate an algorithm for integrating stochastic differential equations under green noise. Utilizing it and the standard methods for computing dynamical systems under red and white noise, we address the problem of synchronization among chaotic oscillators in the presence of common colored noise. We find that colored noise can induce synchronization, but the onset of synchronization, as characterized by the value of the critical noise amplitude above which synchronization occurs, can be different for noise of different colors. A formula relating the critical noise amplitudes among red, green, and white noise is uncovered, which holds for both complete and phase synchronization. The formula suggests practical strategies for controlling the degree of synchronization by noise, e.g., utilizing noise filters to suppress synchronization.

DOI: [10.1103/PhysRevE.79.056210](https://doi.org/10.1103/PhysRevE.79.056210)

PACS number(s): 05.45.Xt, 05.40.Ca, 05.45.Pq

I. INTRODUCTION

The interplay between noise and deterministic nonlinear dynamics often leads to interesting phenomena in physical systems such as noise-induced chaos [1], stochastic resonance [2], coherence resonance [3], and noise-induced synchronization [4–7]. For example, when a dynamical system is in a periodic window so that it permits two coexisting invariant sets, one a periodic attractor and another a nonattracting chaotic set, noise can connect the two sets dynamically, leading to a chaotic attractor (noise-induced chaos). In stochastic resonance, noise can enhance and maximize, often significantly, the response of a nonlinear system to weak signals. In coherence resonance, noise can induce and optimize the temporal regularity of the system dynamics, regardless of the presence of any external signal. For a system of nonlinear oscillators, in the absence of coupling or in the weakly coupling regime where synchronization does not occur, noise applied identically to each oscillator can induce synchronization [4,5]. Numerical and experimental evidence has also been presented for noise-induced chaotic phase synchronization [6–8]. For limit-cycle oscillators, rigorous results have been obtained for noise-induced synchronization [9,10].

The focus of this paper is on synchronization induced by colored noise. Our motivations are twofold. Firstly, in the literature on noise-induced synchronization, Gaussian white noise is often assumed. Such a stochastic process possesses an infinite variance and no time correlation; it thus cannot occur in realistic physical systems. White noise, however, can be viewed as an approximation to “red” noise that possesses an exponentially decaying time correlation. Attention has then been paid to red noise in situations where the issue of time correlation is important [11]. It becomes, however, a tacit working hypothesis in the literature that red noise represents colored noise. In fact, there has been quite limited effort on stochastic processes of other “colors” [12,13] which are characterized by different power spectra, or equivalently, by different autocorrelation functions according to the Wiener-Khinchin theorem. Our interest is thus in the effect of noise of different “colors” on synchronization. Secondly,

stochastic processes of different color are by no means rare but rather, they abound in physical systems such as nonlinear electronic circuits. For example, green noise (see Sec. II for a full description), which exhibits a *negative* component in the autocorrelation function, in contrast to red noise that is positively correlated and white noise that has zero correlation, has been identified in circuit systems [12,13] and in neural networks [14]. A previous study showed that green noise as an internal process can induce abnormal ballistic diffusion due to its vanishing power intensity at zero frequency [15], while white or red noise can only lead to normal diffusion. When green noise is applied externally to some ratchet system exhibiting Brownian motion, net flow of Brownian particles can be induced in the direction opposite to that induced by red noise, and white noise cannot even generate any directional net flow [13]. These works suggest that the effect of the noise color can be quite significant on physical systems. While there is some work on the effect of red noise on synchronization in dynamical systems [16], so far there has been only limited work addressing the role of green noise in synchronization [17]. To our knowledge, there has been no work on the effect of green noise on chaotic synchronization.

In this work, we systematically study the effect of colored noise on the onset of synchronization in chaotic systems. While the less treated case of green noise is our focus, we will consider all three processes: green, red, and white for the reason that the sum of the spectra of red and green noise is the spectrum of white noise and, as a result, their effects on synchronization can be related to each other. Our investigation has indeed revealed such a relation. In particular, let D_W , D_R , and D_G denote the threshold amplitude values for the white, red, and green noise, respectively, above which chaotic synchronization can occur. We find the following relation:

$$\frac{1}{D_R^2} + \frac{1}{D_G^2} = \frac{1}{D_W^2}, \quad (1)$$

which holds for both noise-induced complete synchronization and noise-induced phase synchronization.

In Sec. II, we describe and contrast the properties of white, red, and green noise. While standard numerical algorithms for integrating stochastic differential equations under white and red noise exist, less practiced is integration method for green noise. We thus develop a numerical method to address the integration of dynamical systems under green noise. In Sec. III, we provide evidence and heuristic analysis for relation (1). Discussions are offered in Sec. IV. In Appendix A, we present detailed steps leading to our algorithm to integrate stochastic differential equations under green noise. In Appendix B we describe the Krylov-Bogoliubov averaging method that we have used to validate our proposed numerical algorithm.

II. COLORED NOISE: GENERATION AND INTEGRATION

Red noise can be generated from the following Langevin equation (see, for example, Ref. [11]):

$$\dot{x} = -\gamma x + \gamma \eta, \quad (2)$$

where γ is a positive constant, η represents Gaussian white noise with the properties $\langle \eta \rangle = 0$ and $\langle \eta(t) \eta(t') \rangle = D^2 \delta(t-t')$, and D is the noise amplitude. For $t \rightarrow \infty$ [with the initial condition $\langle x(0) \rangle = 0$], one finds

$$\langle x \rangle = 0, \quad (3)$$

$$\langle x(t)x(t+\tau) \rangle = D^2 \frac{\gamma}{2} e^{-\gamma|\tau|}, \quad (4)$$

$$I_x(\omega) = \frac{D^2}{2\pi} \frac{\gamma^2}{\gamma^2 + \omega^2} \equiv I_R, \quad (5)$$

where I_x is the power spectrum of x and I_R denotes the power spectrum of red noise of amplitude D . From Eq. (4), we see that the autocorrelation function of the stochastic process $x(t)$ decays exponentially, which is characteristic of red noise. Physically, the constant γ thus represents the inverse correlation time of $x(t)$. For dynamical systems under red noise, the second-order Runge-Kutta algorithm [18] is adopted to integrate the set of underlying stochastic differential equations.

In a nonlinear electronic-circuit system, the dynamical variables are voltages and currents, which are often related to one another via time derivatives. When noise is present, the time derivative of the underlying stochastic process appears in the system equations. A simple class of stochastic system taking into account this feature is

$$\dot{x} = -\gamma x - \dot{\eta}, \quad (6)$$

where also η represents Gaussian white noise and $\gamma > 0$ is a constant. Note that the stochastic process $\dot{\eta}$ actually represents violet noise, as its power spectrum has the form $I_{\dot{\eta}} \sim \omega^2$ [19]. After some algebra, we obtain

$$\langle x \rangle = 0, \quad (7)$$

$$\langle x(t)x(t+\tau) \rangle = D^2 \delta(t) - D^2 \frac{\gamma}{2} e^{-\gamma|\tau|}, \quad (8)$$

$$I_x(\omega) = \frac{D^2}{2\pi} \frac{\omega^2}{\gamma^2 + \omega^2} \equiv I_G. \quad (9)$$

The power spectrum of the stochastic process $x(t)$, as represented by Eq. (9), is the defining characteristic of green noise of amplitude D . From Eq. (8), we see that the autocorrelation function of green noise is mostly negative, indicating that the underlying stochastic process is negatively correlated, with γ referred to as the inverse correlation time. Comparison between Eqs. (2) and (6) indicates that both red and green noise can be generated by a linear, first-order stochastic differential equation, when the additive stochastic term corresponds to Gaussian white noise and violet noise, respectively.

While Eq. (6) is motivated by circuit-system considerations, its numerical integration is difficult due to the derivative term of a stochastic process. We thus seek for numerically feasible ways to generate green noise. Consider the following stochastic dynamical system:

$$\begin{cases} \dot{y} = f(y) + \xi - \eta \\ \dot{\xi} = -\gamma \xi + \gamma \eta. \end{cases} \quad (10)$$

We see from Eq. (2) that ξ is a stochastic process that generates red noise. Suppose η represents Gaussian white noise. The power spectrum of the stochastic process $\xi - \eta$ can be calculated as

$$\begin{aligned} I_{\xi-\eta} &= [\tilde{\xi}(\omega) - \tilde{\eta}(\omega)][\tilde{\xi}^*(\omega) - \tilde{\eta}^*(\omega)] = \frac{D^2}{2\pi} \left[\frac{\gamma}{\gamma + i\omega} - 1 \right] \\ &\times \left[\frac{\gamma}{\gamma - i\omega} - 1 \right] = \frac{D^2}{2\pi} \frac{\omega^2}{\gamma^2 + \omega^2}, \end{aligned}$$

which is characteristic of green noise. Since the power spectrum of white noise η is a constant: $I_\eta = D^2/2\pi \equiv I_W$, we have $I_G + I_R = I_W$. To solve Eq. (10) numerically, we have developed the following second-order Runge-Kutta algorithm:

$$\begin{cases} y(t + \Delta t) = y(t) + \frac{1}{2} \Delta t (F_1 + F_2) - D \sqrt{\Delta t} \psi, \\ \xi(t + \Delta t) = \xi(t) + \frac{1}{2} \Delta t (H_1 + H_2) + D \gamma \sqrt{\Delta t} \psi, \end{cases} \quad (11)$$

where $\psi \sim N(0, 1)$ is a standard Gaussian random number and

$$H_1 = -\gamma \xi(t),$$

$$H_2 = -\gamma [\xi(t) + \Delta t H_1 + D \gamma \sqrt{\Delta t} \psi],$$

$$F_1 = f[y(t)] + \xi(t),$$

$$F_2 = f[y(t) + \Delta t F_1 - D \sqrt{\Delta t} \psi] - H_2 / \gamma.$$

Details of the derivation of this algorithm can be found in Appendix A. Note that our algorithm is naturally reduced to that dealing with red noise if there is no white noise term in the evolutionary equation of y in Eq. (10), and to that for white noise if Eq. (10) contains no ξ -related terms [18]. Note also that both green and red noise are limiting cases of broad-band noise and, hence, the general algorithm that deals

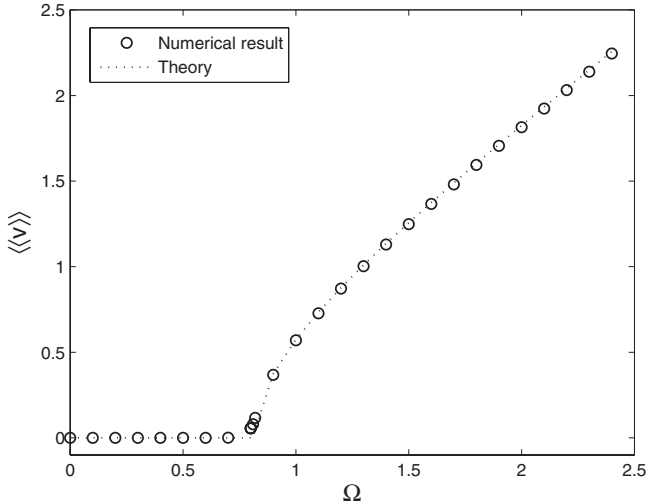


FIG. 1. For the analytically solvable model Eq. (12) under green noise, the analytically predicted average velocity $\langle\langle v \rangle\rangle$ as a function of Ω versus numerically obtained result from our algorithm (11). Parameters are $D=2$ and $\gamma=5$.

with broad-band noise in [20] can in principle be used to integrate dynamical systems under colored noise.

To validate our algorithm, we consider the following model that can be analytically solved by using the Krylov-Bogoliubov averaging method [12]:

$$\dot{y} = f(y) + \varepsilon, \tag{12}$$

where $f(y) = \Omega - \sin y$ and ε denotes green noise. Details of the procedure to solve this equation are provided in Appendix B, and here we just present the result. An example of the time-averaged velocity $\langle\langle v \rangle\rangle \equiv \langle\langle \dot{y} \rangle\rangle$ is plotted in Fig. 1 as a function of Ω by using our algorithm (11). The parameters used are $D=2$ and $\gamma=5$. The numerical result can be compared with analytical result that $\langle\langle v \rangle\rangle = 0$ for $|\Omega| < \Omega_{\text{eff}}$ and $\langle\langle v \rangle\rangle = \sqrt{\Omega^2 - \Omega_{\text{eff}}^2}$ for $|\Omega| > \Omega_{\text{eff}}$, where $\Omega_{\text{eff}} = \exp(-D^2/4\gamma) \approx 0.8187$. We observe an excellent agreement between the result from our algorithm and the analytic prediction, thereby validating our algorithm (11) to integrate stochastic differential equations under green noise.

III. CHAOTIC SYNCHRONIZATION INDUCED BY COLORED NOISE

We consider a set of *uncoupled* chaotic oscillators, each driven by a common noise source, as shown schematically in Fig. 2. Previous works have demonstrated that, when noise is of the Gaussian white type, synchronization among the oscillators can arise as the noise amplitude is increased through a critical value, say D_w [6]. Our focus is on whether colored noise can induce synchronization and if yes, the value of the critical noise amplitude required for synchronization. We shall study red and green noise, as their spectral properties are different but are complementary with respect to the spectrum of white noise. Under noisy driving, each chaotic oscillator can be regarded as a subsystem in a stochastic system that consists of the noise source and the oscillator itself. Ac-

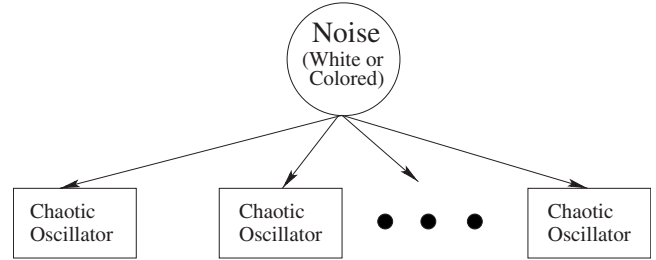


FIG. 2. Schematic illustration of the setting for studying noise-induced synchronization. Each chaotic oscillator can be regarded as a subsystem and its Lyapunov spectrum under noisy driving can be calculated. Complete synchronization and phase synchronization occur when the largest Lyapunov exponent and the originally null Lyapunov exponent become negative, respectively.

ording to the criterion by Pecora and Carroll [21], when the largest Lyapunov exponent λ_1 of the subsystem is negative, synchronization occurs among all oscillators. We shall then compute λ_1 as a function of the noise amplitude and determine the critical colored-noise amplitudes, D_R and D_G , required for synchronization if it occurs. For phase synchronization, the criterion is to examine the behavior of the null Lyapunov exponent in the underlying deterministic oscillator as noise is turned on. In particular, let $\lambda_2=0$ be the exponent when noise is absent. As the noise amplitude is increased from zero, λ_2 can become negative. We shall determine the onset of phase synchronization by the zero crossing of λ_2 .

We choose the classical Lorenz system [22] as our primary model chaotic oscillator, as described by $\dot{x} = 10(y-x)$, $\dot{y} = 28x - y - xz$, and $\dot{z} = xy - (8/3)z$. To be concrete, we assume that noisy driving occurs in the y equation. Typical trajectories of the system under white, red, or green noise are shown in Fig. 3. For red or green noise, the parameter γ in their spectra is chosen to be 3, and the noise amplitude D is chosen to be 20 for all types of noise. Figures 4(a) and 4(b) show λ_1 versus the noise amplitude D for red and green noise,

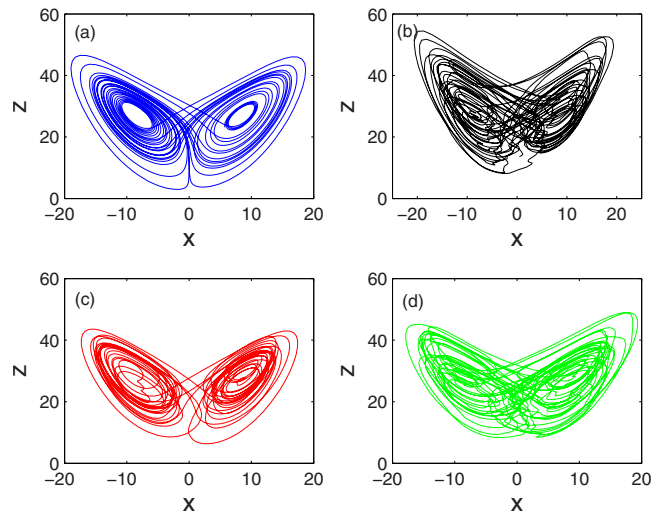


FIG. 3. (Color online) Typical trajectories of the chaotic Lorenz oscillator under (a) no noise, (b) white noise with $D=20$, (c) red noise with $\gamma=3$ and $D=20$, and (d) green noise with $\gamma=3$ and $D=20$.

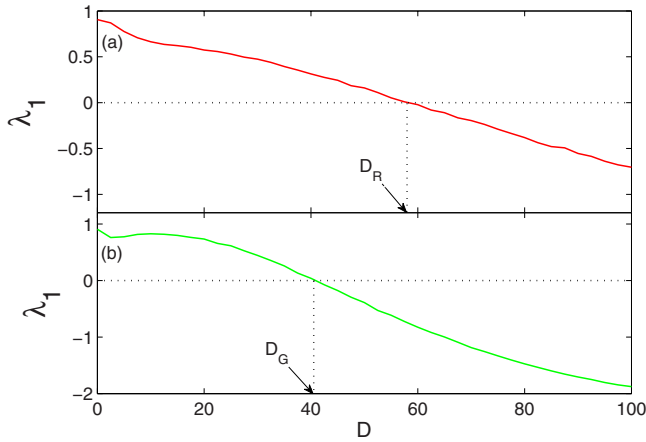


FIG. 4. (Color online) For the classical Lorenz chaotic oscillator, λ_1 versus D for (a) red noise and (b) green noise. The parameter γ in the power spectrum of noise is 3. In both cases, noise can induce synchronization if its amplitude is sufficiently large. We observe $D_R \approx 58$ and $D_G \approx 41$.

respectively ($\gamma=3$ for both types of noise). We see that for sufficiently large values of D , λ becomes negative, indicating that both red and green noise can induce chaotic synchronization. However, the critical noise amplitudes required for synchronization are quite different for red and green noise, as indicated by the arrows in Figs. 4(a) and 4(b). In particular, we find $D_R \approx 58$ and $D_G \approx 41$. If noise is white, we find $D_W \approx 33.3$. We observe the approximate relation: $1/D_R^2 + 1/D_G^2 \approx 1/D_W^2$. In fact, this approximation relation holds for other values of γ , as shown in Fig. 5, where γ is varied over nearly 4 orders of magnitude. Note that, since white noise has a flat power spectrum, D_W does not depend on γ . Figure 5(a) shows D_R and D_G versus γ , and D_W is indicated by the horizontal dotted line. Figure 5(b) shows the quantity \bar{D} , defined as $1/\bar{D}^2 \equiv 1/D_R^2 + 1/D_G^2$, as a function of γ . We see that

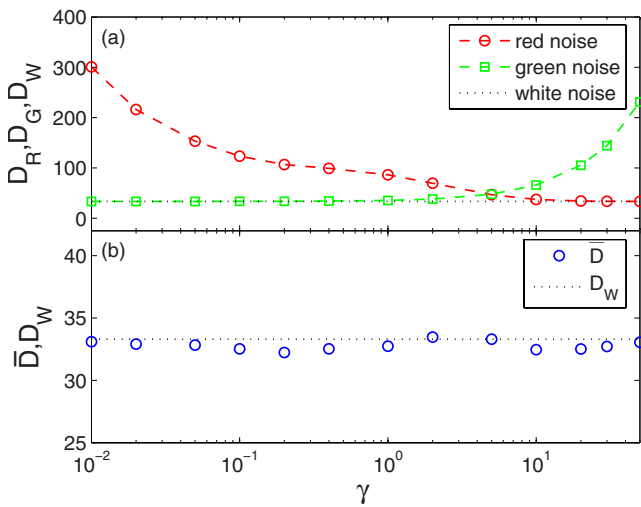


FIG. 5. (Color online) For the classical Lorenz chaotic oscillator, (a) D_R and D_G versus γ , where the horizontal dotted line denotes the value of D_W , and (b) The value of \bar{D} as defined by $1/\bar{D}^2 \equiv 1/D_R^2 + 1/D_G^2$ versus γ . It can be seen that \bar{D} is approximately constant and in fact, $\bar{D} \approx D_W$ for all values of γ tested.

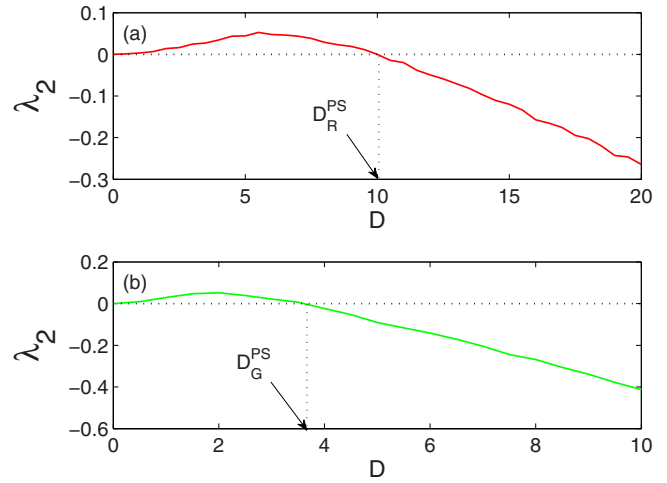


FIG. 6. (Color online) For the classical Lorenz chaotic oscillator, λ_2 versus D for (a) red noise and (b) green noise, where $\gamma=3$. In both cases, noise can induce chaotic phase synchronization. We observe $D_R^{PS} \approx 9.9$ and $D_G^{PS} \approx 3.6$.

\bar{D} is approximately constant and it is in fact quite close to D_W for all values of γ examined.

Does relation (1) hold for chaotic phase synchronization? Our computations indicate that for the Lorenz oscillator, it apparently holds. In particular, Figs. 6(a) and 6(b) show the deterministically null subsystem Lyapunov exponent λ_2 versus the noise amplitude for red and green noise, respectively, for $\gamma=3$. We observe that colored noise can induce chaotic phase synchronization. For red (green) noise, this occurs for $D > D_R^{PS} \approx 9.9$ ($D > D_G^{PS} \approx 3.6$). In both cases, for noise amplitude between zero and the critical value, λ_2 is in fact positive. This has been understood as being due to the destruction of the neural direction by noise as the trajectory passes through the neighborhood of the unstable steady state that dynamically separates the left and the right scroll in the Lorenz system [23]. For white noise driving, we find $D_W^{PS} \approx 3.4$. We again observe that $1/(D_R^{PS})^2 + 1/(D_G^{PS})^2 \approx 1/(D_W^{PS})^2$. Figure 7(a) shows D_R^{PS} and D_G^{PS} versus γ , and relation (1) apparently holds for all values of γ tested.

We have also tested other chaotic oscillators, such as the chaotic Rössler oscillator given by $\dot{x} = -y - z$, $\dot{y} = x + 0.15y + n_c$, and $\dot{z} = 0.4 + z(x - 8.5)$, where n_c denotes the stochastic process that generates colored noise of interest. Typical trajectories of the system under different kinds of noise are shown in Fig. 8. That colored noise can induce chaotic (phase) synchronization and relation (1) have also been observed in the Rössler oscillator as shown in Figs. 9 and 10.

We now provide a heuristic justification for Eq. (1). First, Eq. (1) holds in the limiting cases of γ . Note that, for $\gamma \rightarrow \infty$, we have $\gamma e^{-\gamma|\tau|/2} \rightarrow \delta(\tau)$. Thus, for large values of γ , the correlation property of red noise tends to that of white noise, while the autocorrelation function associated with green noise tends to zero. For small values of γ , the opposites occur. We thus expect $D_R \rightarrow D_W$ and $D_G \rightarrow \infty$ as $\gamma \rightarrow \infty$. For $\gamma \rightarrow 0$, we have $D_R \rightarrow \infty$ and $D_G \rightarrow D_W$. Thus, Eq. (1) holds for both the limiting cases of large and near zero values of γ . Second, although we are unable to calculate D_W , D_R , or D_G theoretically at the present, a phenomenological

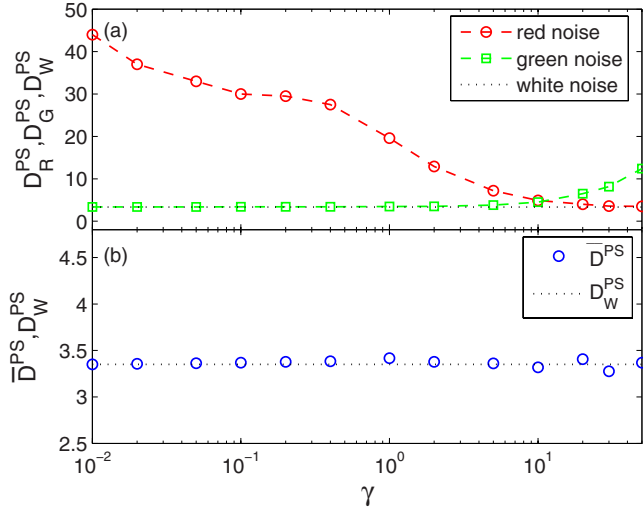


FIG. 7. (Color online) For the classical Lorenz chaotic oscillator, (a) D_R^{PS} and D_G^{PS} versus γ , where the horizontal dotted line denotes the value of D_W^{PS} , and (b) value of \bar{D}^{PS} as defined by $1/(\bar{D}^{PS})^2 \equiv 1/(D_R^{PS})^2 + 1/(D_G^{PS})^2$ versus γ . It can be seen that \bar{D}^{PS} is approximately constant and in fact, $\bar{D}^{PS} \approx D_W^{PS}$ for all values of γ tested in a wide range.

understanding of Eq. (1) can be obtained based on the observation that $I_R + I_G = I_W$. In particular, any external noise can be regarded as random perturbation to the deterministic chaotic oscillator. To make uncoupled oscillators synchronized, certain amount of “energy,” denoted by E , is needed. Heuristically, we can write

$$E \sim \int I_i(\omega)\rho(\omega)d\omega, \quad (13)$$

where i denotes a particular type of colored noise, $I_i(\omega)$ is the power spectrum of the noise, and $\rho(\omega)$ is a weighting func-

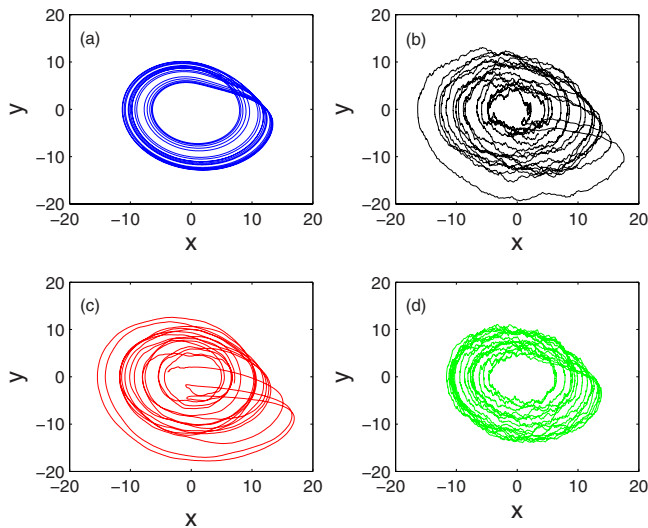


FIG. 8. (Color online) Typical trajectories of the chaotic Rössler oscillator under (a) no noise, (b) white noise of amplitude $D=1.5$, (c) red noise characterized by $\gamma=3$ and $D=1.5$, (d) green noise characterized by $\gamma=3$ and $D=1.5$.

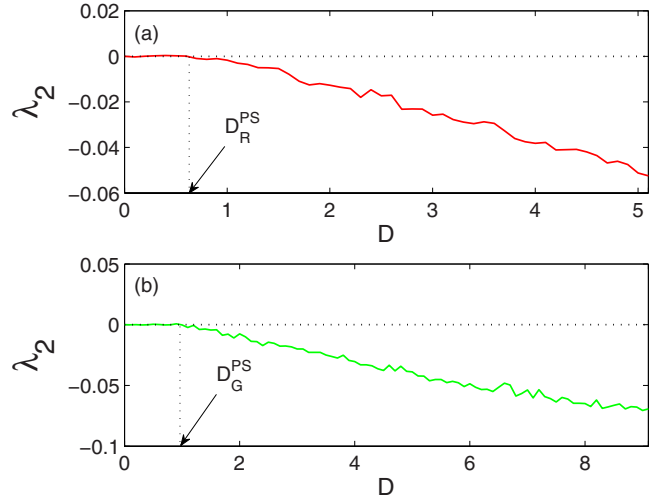


FIG. 9. (Color online) For the noise-driven chaotic Rössler oscillator, λ_2 versus D for (a) red noise and (b) green noise, where $\gamma=3$. In both cases, noise can induce chaotic phase synchronization.

tion determined by the underlying chaotic system. The intuitive idea is that, in order for certain collective behavior (e.g., synchronization) to occur, the energy of the system should at least have the value as given by Eq. (13). Moreover, such energy is provided weightedly by the external noise; the weight of the noise’s each harmonic mode is determined by the property of the chaotic system. The power spectra of red and green noise are given by Eq. (5) and Eq. (9), respectively, and the power spectrum of white noise is $I_W = D^2/2\pi$. Equation (13) thus leads to $E/D_W^2 = E/D_R^2 + E/D_G^2$, which is Eq. (1). While this explanation is heuristic, it provides insights into the general phenomenon of chaotic synchronization as induced by colored noise.

IV. CONCLUSION AND DISCUSSION

Motivated by the consideration that existing works on noise-induced synchronization have mostly assumed Gauss-

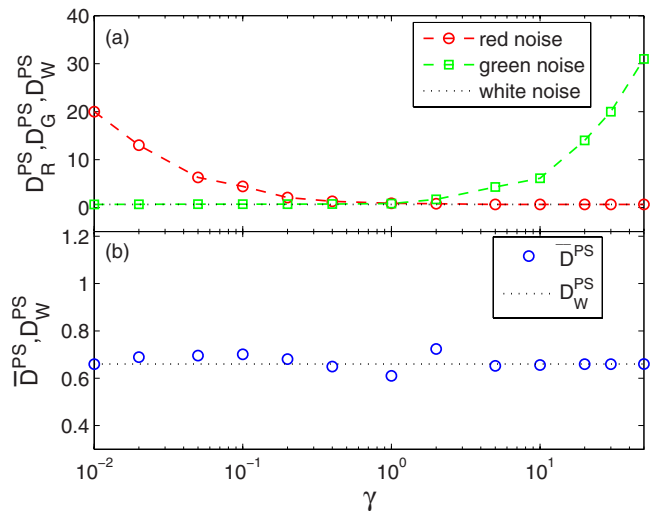


FIG. 10. (Color online) For the chaotic Rössler oscillator, (a) D_R^{PS} and D_G^{PS} versus γ , where the horizontal dotted line denotes the value of D_W^{PS} , and (b) value of \bar{D}^{PS} as defined by $1/(\bar{D}^{PS})^2 \equiv 1/(D_R^{PS})^2 + 1/(D_G^{PS})^2$ versus γ .

ian white noise but colored noise can arise commonly in realistic physical systems, we have investigated the onset of synchronization among chaotic oscillators as driven by common colored noise. We focus on red and green noise, whose power spectra are complementary to each other. While standard numerical methods for integrating stochastic differential equations under white and red noise are available, integrating differential equations under green noise is less practiced. As a prerequisite to addressing the problem of synchronization, we have developed an efficient numerical algorithm to deal with stochastic equations under green noise and validated it using an analytically solvable model. The problem of colored-noise-induced synchronization has then been investigated systematically by using well-known chaotic oscillators. Both complete synchronization and phase synchronization have been taken into account, based on the calculations of the noise-driven Lyapunov exponents as functions of the noise amplitude. Our main result is Eq. (1), a quantitative expression relating the synchronization thresholds of red, green, and white noise. The result indicates that the critical amplitude required for synchronization is generally smaller for white noise as compared with colored noise. A practical implication is that, in situations where synchronization is undesirable (e.g., in certain biomedical applications such as epileptic seizures), a simple control strategy is to place filters in the system so as to make the noise source as colored as possible.

ACKNOWLEDGMENTS

Y.C.L. was supported by ONR under Grant No. N00014-08-1-0627. Y.W.'s visit to Arizona State University was sponsored by the State Scholarship Fund of China. Y.W. and Z.G.Z. were partially supported by NNSFC Grant No. 10875011, the 973 Program Grant No. 2007CB814805, the Foundation of Doctoral Training Grant No. 20060027009.

APPENDIX A

Here we sketch our proposed second-order stochastic Runge-Kutta algorithm for integrating differential equations under green noise. Our basic idea is similar to that in [18] where red or white noise is treated. A general algorithm dealing with broad-band noise, of which green or red noise is a limiting case, can be found in [20].

Integrating Eq. (10) from time 0 to time Δt , we obtain

$$y(\Delta t) = y_0 + \int_0^{\Delta t} f[y(t')]dt' + \int_0^{\Delta t} \xi(t')dt' - \int_0^{\Delta t} \eta(t')dt',$$

$$\xi(\Delta t) = \xi_0 + \int_0^{\Delta t} [-\gamma\xi(t')]dt' + \int_0^{\Delta t} \gamma\eta(t')dt'. \quad (\text{A1})$$

Defining

$$\Gamma_0(t) \equiv \int_0^t \eta(t')dt',$$

$$\Gamma_i(t) \equiv \int_0^t \Gamma_{i-1}(t')dt', \quad i = 1, 2, \dots,$$

and using the identity [18]

$$\langle \Gamma_m(t)\Gamma_n(t) \rangle = D^2 \frac{t^{m+n+1}}{m!n!(m+n+1)},$$

we can expand Eq. (A1) about y_0 to $(\Delta t)^2$. We have

$$y(\Delta t) = y_0 + f_0\Delta t + \frac{1}{2}f_0f_0'(\Delta t)^2 + \frac{1}{2}\xi_0f_0'(\Delta t)^2 + \xi_0\Delta t - \frac{1}{2}\gamma\xi_0(\Delta t)^2 + S_y,$$

$$\xi(\Delta t) = \xi_0 - \gamma\xi_0\Delta t + \frac{1}{2}\gamma^2\xi_0(\Delta t)^2 + S_\xi,$$

where $f_0 = f(y_0)$, and

$$S_y = -\Gamma_0(\Delta t) + \frac{1}{2}f_0'' \int_0^{\Delta t} dt' \Gamma_0^2(t') + \gamma\Gamma_1(\Delta t) - f_0'\Gamma_1(\Delta t),$$

$$S_\xi = \gamma\Gamma_0(\Delta t) - \gamma^2\Gamma_1(\Delta t).$$

After some algebra, we get the mean and variance of S_y and S_ξ to the order of $(\Delta t)^2$:

$$\langle S_y \rangle = \frac{D^2}{4}f_0''(\Delta t)^2,$$

$$\langle S_y^2 \rangle = D^2\Delta t - D^2\gamma(\Delta t)^2 + D^2f_0'(\Delta t)^2,$$

$$\langle S_\xi \rangle = 0,$$

$$\langle S_\xi^2 \rangle = D^2\gamma^2\Delta t - D^2\gamma^3(\Delta t)^2. \quad (\text{A2})$$

Parallely, starting directly from Eq. (10) by using a second-order Runge-Kutta method, we have

$$y(\Delta t) = y_0 + \frac{1}{2}\Delta t(F_1 + F_2) - D\sqrt{\Delta t}\phi_0,$$

$$\xi(\Delta t) = \xi_0 + \frac{1}{2}\Delta t(H_1 + H_2) + D\gamma\sqrt{\Delta t}\phi_0, \quad (\text{A3})$$

where

$$H_1 = -\gamma(\xi_0 + D\gamma\sqrt{\Delta t}\phi_1),$$

$$H_2 = -\gamma(\xi_0 + \Delta t H_1 + D\gamma\sqrt{\Delta t}\phi_2),$$

$$F_1 = f(y_0 - D\sqrt{\Delta t}\phi_1) + \xi_0 + D\gamma\sqrt{\Delta t}\phi_1,$$

$$F_2 = f(y_0 + \Delta t F_1 - D\sqrt{\Delta t}\phi_2) + \xi_0 + \Delta t H_1 + D\gamma\sqrt{\Delta t}\phi_2,$$

and ϕ_0 , ϕ_1 , and ϕ_2 are three independent standard Gaussian random numbers with zero mean and unit variance. We then expand Eq. (A3) about y_0 to order $(\Delta t)^2$ to obtain

$$y(\Delta t) = y_0 + f_0 \Delta t + \frac{1}{2} f_0 f_0' (\Delta t)^2 + \frac{1}{2} f_0' \xi_0 (\Delta t)^2 + \xi_0 \Delta t - \frac{1}{2} \gamma \xi_0 (\Delta t)^2 + S_y',$$

$$\xi(\Delta t) = \xi_0 - \gamma \xi_0 \Delta t + \frac{1}{2} \xi_0 \gamma^2 (\Delta t)^2 + S_\xi',$$

where

$$S_y' = -D\sqrt{\Delta t} \phi_0 - \frac{1}{2} D(f_0' - \gamma)(\sqrt{\Delta t})^3 \phi_1 + \frac{D^2}{4} f_0'' (\Delta t)^2 \phi_1^2 - \frac{1}{2} D(f_0' - \gamma)(\sqrt{\Delta t})^3 \phi_2 + \frac{D^2}{4} f_0'' (\Delta t)^2 \phi_2^2,$$

$$S_\xi' = D\gamma\sqrt{\Delta t} \phi_0 - \frac{1}{2} D\gamma^2 (\sqrt{\Delta t})^3 \phi_1 - \frac{1}{2} D\gamma^2 (\sqrt{\Delta t})^3 \phi_2.$$

The means and the variances of S_y' and S_ξ' are calculated to be

$$\langle S_y' \rangle = \frac{D^2}{4} f_0'' (\Delta t)^2 \langle \phi_1^2 \rangle + \frac{D^2}{4} f_0'' (\Delta t)^2 \langle \phi_2^2 \rangle,$$

$$\langle S_y'^2 \rangle = D^2 \Delta t \langle \phi_0^2 \rangle + D^2 (f_0' - \gamma) (\Delta t)^2 \langle \phi_0 (\phi_1 + \phi_2) \rangle,$$

$$\langle S_\xi' \rangle = 0,$$

$$\langle S_\xi'^2 \rangle = D^2 \gamma^2 \Delta t \langle \phi_0^2 \rangle - D^2 \gamma^3 (\Delta t)^2 \langle \phi_0 (\phi_1 + \phi_2) \rangle. \quad (\text{A4})$$

Equating Eq. (A2) to Eq. (A4) leads to

$$\langle \phi_0^2 \rangle = 1,$$

$$\langle \phi_1^2 \rangle + \langle \phi_2^2 \rangle = 1,$$

$$\langle \phi_0 (\phi_1 + \phi_2) \rangle = 1.$$

Since there are three equations and three unknowns, it is possible to define a standard Gaussian random number ψ such that $\phi_i = a_i \psi$, $i=0,1,2$. To maintain the structure of the Runge-Kutta algorithm, we can conveniently choose $a_0 = a_2 = 1$ and $a_1 = 0$. These considerations lead to the algorithm as represented by Eq. (11).

APPENDIX B

The standard Fokker-Planck equation can be used to analyze dynamical systems under white noise. However, when noise is colored (especially green), the equation becomes quite complicated. For example, the Fokker-Planck equation

associated with the Langevin equation Eq. (10) under green noise reads

$$\frac{\partial P}{\partial t} = -\frac{\partial}{\partial y} [f(y) - \gamma \xi] P + \gamma \frac{\partial (\xi P)}{\partial \xi} + D^2 \left(\frac{\partial^2 P}{\partial y^2} + \frac{\partial^2 P}{\partial \xi^2} \right) + 2D^2 \frac{\partial^2 P}{\partial y \partial \xi}.$$

To gain theoretical insights into the properties of dynamical systems under green noise, the Krylov-Bogoliubov averaging method is useful [12]. The application of this method requires the existence of two time scales, fast and slow, in the system. The averaging process picks out the slow motion that is assumed to dominate the evolution of the system. In Eq. (12), the natural fast time scale is one determined by noise correlation time $1/\gamma$. The condition under which the averaging method can be applied is then $1 \gg 1/\gamma$.

Equation (12) can be rewritten as

$$\hat{L}z = \Omega - \sin(z + \xi), \quad (\text{B1})$$

where $\hat{L} \equiv d/dt$, $z = y - \xi$, and ξ is a stationary process satisfying $\hat{L}\xi = \varepsilon$. Taking time average of Eq. (B1) over a sufficiently long time interval T ($T \gg 1/\gamma$), we obtain

$$\hat{L}\bar{z} = \langle \Omega - \sin(\bar{z} + \xi) \rangle, \quad (\text{B2})$$

where \bar{z} is the time average of z within T , and it can be regarded as constant in the right-hand side of Eq. (B2) when the ensemble average is taken. (Here ergodicity of the dynamics is assumed so that time average can be replaced by ensemble average.) Since $\bar{z} = \bar{y} = \langle y \rangle + o(1/\gamma)$, Eq. (12) becomes

$$\hat{L}\langle y \rangle = \langle \Omega - \sin(\langle y \rangle + \xi) \rangle = \Omega - \Omega_{\text{eff}} \sin(\langle y \rangle), \quad (\text{B3})$$

where $\Omega_{\text{eff}} = \langle \cos \xi \rangle = \exp(-D^2/4\gamma)$.

Equation (B3) is the Adler equation, one of the simplest forms of averaged phase equations arising in the study of synchronization of periodic oscillators by periodic external driving force [5], where properties of the solutions to the Adler equation have been analyzed. For example, for $|\Omega| < \Omega_{\text{eff}}$, the system has one stable fixed point, and so the long time average velocity is $\langle \langle \dot{y} \rangle \rangle = 0$. While for $|\Omega| > \Omega_{\text{eff}}$, the solution to Eq. (B3) can be formally written as

$$\int^y \frac{dy}{\Omega - \Omega_{\text{eff}} \sin y} = t \equiv \frac{y}{\Omega_y},$$

where Ω_y is the frequency of y , which can be calculated as

$$\Omega_y = 2\pi \left(\int_0^{2\pi} \frac{dy}{\Omega - \Omega_{\text{eff}} \sin y} \right)^{-1} = \sqrt{\Omega^2 - \Omega_{\text{eff}}^2}. \quad (\text{B4})$$

This leads to $\langle \langle \dot{y} \rangle \rangle = \Omega_y = \sqrt{\Omega^2 - \Omega_{\text{eff}}^2}$, a property that we have used to validate our numerical algorithm Eq. (11).

- [1] See, for example, A. Hamm, T. Tél, and R. Graham, *Phys. Lett. A* **185**, 313 (1994); L. Billings and I. B. Schwartz, *J. Math. Biol.* **44**, 31 (2002); Y.-C. Lai, Z. Liu, L. Billings, and I. B. Schwartz, *Phys. Rev. E* **67**, 026210 (2003).
- [2] See, for example, K. Wiesenfeld and F. Moss, *Nature (London)* **373**, 33 (1995); L. Gammaitoni, P. Hänggi, P. Jung, and F. Marchesoni, *Rev. Mod. Phys.* **70**, 223 (1998).
- [3] See, for example, D. Sigeti and W. Horsthemke, *J. Stat. Phys.* **54**, 1217 (1989); A. S. Pikovsky and J. Kurths, *Phys. Rev. Lett.* **78**, 775 (1997); Z. Liu and Y.-C. Lai, *ibid.* **86**, 4737 (2001).
- [4] See, for example, A. S. Pikovsky, *Radiophys. Quantum Electron.* **27**, 576 (1984); P. Houry, M. A. Lieberman, and A. J. Lichtenberg, *Phys. Rev. E* **54**, 3377 (1996); L. Yu, E. Ott, and Q. Chen, *Phys. Rev. Lett.* **65**, 2935 (1990).
- [5] A. S. Pikovsky, M. Rosenblum, and J. Kurths, *Synchronization: A Unified Approach to Nonlinear Science* (Cambridge University Press, Cambridge, 2001).
- [6] C. Zhou and J. Kurths, *Phys. Rev. Lett.* **88**, 230602 (2002); C. Zhou, J. Kurths, I. Z. Kiss, and J. L. Hudson, *ibid.* **89**, 014101 (2002).
- [7] A. Uchida, R. McAllister, and R. Roy, *Phys. Rev. Lett.* **93**, 244102 (2004).
- [8] K. Park, Y.-C. Lai, S. Krishnamoorthy, and A. Kandangath, *Chaos* **17**, 013105 (2007).
- [9] J.-N. Teramae and D. Tanaka, *Phys. Rev. Lett.* **93**, 204103 (2004).
- [10] D. S. Goldobin and A. Pikovsky, *Phys. Rev. E* **71**, 045201(R) (2005).
- [11] S. Mangioni, R. Deza, H. S. Wio, and R. Toral, *Phys. Rev. Lett.* **79**, 2389 (1997).
- [12] S. A. Guz and M. V. Sviridov, *Phys. Lett. A* **240**, 43 (1998); *Chaos* **11**, 605 (2001).
- [13] J.-D. Bao and S. J. Liu, *Phys. Rev. E* **60**, 7572 (1999).
- [14] R. Moreno, J. de la Rocha, A. Renart, and N. Parga, *Phys. Rev. Lett.* **89**, 288101 (2002); H. Câteau and A. D. Reyes, *ibid.* **96**, 058101 (2006).
- [15] J.-D. Bao and Y.-Z. Zhuo, *Phys. Rev. Lett.* **91**, 138104 (2003).
- [16] K. Yoshimura, I. Valiusaityte, and P. Davis, *Phys. Rev. E* **75**, 026208 (2007); B. C. Bag, K. G. Petrosyan, and C.-K. Hu, *ibid.* **76**, 056210 (2007).
- [17] S. A. Guz, Yu. G. Krasnikov, and M. V. Sviridov, *Dokl. Akad. Nauk* **365**, 34 (1999); S. A. Guz, R. Mannella, and M. V. Sviridov, *J. Comm. Tech. Electronics* **50**, 1281 (2005).
- [18] R. L. Honeycutt, *Phys. Rev. A* **45**, 600 (1992); **45**, 604 (1992).
- [19] A concrete example where violet noise naturally arises is in circuit systems. Consider the simple situation where a random voltage signal passes through a capacitor. Assuming the voltage fluctuations are described by a Gaussian process (white noise), the current will contain a term that is the time derivative of the Gaussian process. For a simple circuit system of a resistor, a capacitor, and a white voltage source connected in series, the equation for the current is nothing but Eq. (6). As we can see, the current itself is a stochastic process characteristic of green noise.
- [20] J.-D. Bao, *J. Stat. Phys.* **114**, 503 (2004).
- [21] L. M. Pecora and T. L. Carroll, *Phys. Rev. Lett.* **64**, 821 (1990).
- [22] E. N. Lorenz, *J. Atmos. Sci.* **20**, 130 (1963).
- [23] Z. Liu, Y.-C. Lai, and M. A. Matías, *Phys. Rev. E* **67**, 045203(R) (2003).